中国科学院文献情报系统先进能源情报网

2017 年第 1 期

# 强磁场科学与技术研究动态

主办单位： 中国科学院合肥物质科学研究院信息中心

中 国 科 学 院 强 磁 场 科 学 中 心

# 本期要览

## ✧ 最新资讯

### 美国强磁场创造了混合磁体新的记录

在经过十年的准备，设计和建设之后，美国强磁场实验室成功测试了一台33 吨重的串联混合磁体装置。在 2016 年 12 月 8 日，装置达到了其设计指标: 36T。这一里程碑式的发现打开了一扇发现之门，不仅使物理学家能够使用最强的磁场，而且首次向生物学家和化学家提供了可以利用的强磁场条件。这是十年时间，120000 个工作时，1870 万美元的辉煌成果。

### 迷你磁体的世界记录

2017 年 1 月 18 日，美国强磁场实验室研制的一台能放在手掌上的磁体创造了一项新的世界记录，磁体由高温超导带材绕制而成，中心磁场达到了 11.3T，结合水冷磁体提供的 31.2T 背景磁场。该磁体能够工作在 42.5T 的磁场条件下，实现了两项记录: 首先，42.5T 是目前超导磁体实现运行的最高磁场; 再者，42.5T 也是高温超导磁体在背景磁场下运行的最高记录。

### 230 万欧元用于研究新型金属

荷兰基础物质研究基金会批准了 1510 万欧元启动了七个新的研究项目。其中 230 万欧元用于新型金属研究项目。该项目汇集了来自奈梅亨大学和阿姆斯特丹大学的弦理论家，量子多体理论家，凝聚态物理学家等。计划由奈梅亨强磁场实验室的负责人 Nigel Hussy 教授领衔，将研究新型金属材料的起源。新型金属不符合标准的金属行为模型，是现代物理学中最基本和最紧迫的问题之一。新型金属研究项目将确定这种新型金属是否代表了一种新的量子临界相。同时，该项目还将建立世界第一台光学装置，用于测量新型金属在 35T 以上磁场下的光导性。新型金属行为的物理识别对发展高温超导的相干理论非常重要，这将为我们追求更高转变温度的超导材料提供指导作用。

## ✧ 强磁场设备研制

### 用于传导冷却高场磁体的高温超导内插线圈的交流损耗分析

基于平板近似假设，针对一台用于 25T 无液氦磁体的高温超导内插线圈，对其在励磁情况下的交流损耗进行了数值分析。该高温超导内插磁体由 68 个镀层导体绕制的饼组成，将提供 11.5T 中心磁场，其外部的低温超导磁体将提供 14T 中心磁场。磁体由制冷机冷却，60 分钟励磁至 25.5T，局部磁场被分为轴向分量

和径向分量。在开始励磁时，轴向磁场引起的交流损耗占主要部分，而当径向磁场引起的交流损耗变成主要来源后，总损耗将随时间线性增加。

### 36T 串联混合磁体的设计和组装

由水冷磁体和超导磁体组成的36T混合磁体的组装已在佛罗里达的美国强磁场实验室完成，装置主要用于 NMR 研究。该混合磁体由一台 23T 的水冷磁体和一台 13T 的超导磁体串联而成，共用一台电源，工作电流为 20kA。系统将为凝聚态 NMR 的研究提供 1.53GHZ 的新纪录，在 1cm 的球空间内提供 1ppm 的磁场均匀度。水冷磁体由四个同轴 Florida-Bitter 磁体组成，电源功率 14MW。超导磁体由 4.5K，3.5bar 的超临界氦迫流冷却。超导磁体失超保护系统由两套完全独自的电路组成。目前，水冷磁体已完成测试，超导磁体已降至 4.5T，正在准备混合磁体的调试。

### 法国混合磁体中涡流屏蔽的作用和影响

在法国新的混合磁体中，一个具有很好导电性能的保护屏被安装在水冷磁体和超导磁体之间。他的作用是减少水冷磁体故障时超导磁体中感应的交流损耗，通过缓和磁通变化避免超导磁体失超。由于铜材料的存在，保护屏中的感应电流将会很大，这也正是好的屏蔽效果的缺点。尤其在一半水冷磁体烧毁的极端条件下，这些电流将导致很大的洛伦兹力。同时，失超探测系统也必须特殊设计，以便处理屏蔽对感应电压的影响。

## ✧ 强磁场与生物医学

第一篇（A new twist on DNA）利用了美国强磁场中心的氢氘交换，研究了 DNA 合成过程中 DNA 和解旋酶的结构细节信息，属于基础生物学研究范围。（2016 年发表在生物学二区杂志 Journal of Biological Chemistry，属于 Nature Index 杂志，影响因子约为 4 分）。

第二篇（New technique for detecting brain tumors）文章还没发表，重要程度较高。利用了美国强磁场中心的大口径 21.1T MRI，合成了 $^{17}O$ 标记的蔗糖，利用肿瘤组织糖消耗较高的特性，首次在带有脑部肿瘤的活体大鼠脑部观测到了较高分辨率（1mm3）的肿瘤组织成像。有望成为一种新型的肿瘤成像方法。

## ✧ 强磁场与材料科学[1]

电子具有电荷与自旋。在石墨烯和单层 WS2 等化合物中，由于晶体结构对

[1] 本节所标引数字为正文英文文章序号。

称性的问题，还会产生手性的问题。科学家们精巧地设计了一个具有轻微错位的单层石墨烯/氮化硼/单层石墨烯的三明治异质结，并利用荷兰和法国欧洲强磁场设施在面内施加 30T 强磁场引起的洛伦兹力，使得电子可以轻松的穿越绝缘氮化硼层，从而可以通过调节磁场角度选择不同手性的电子[1,2]。科学家们还使用时间分辨的科尔效应，可以分辨不同手性电子引起的不同的激发，并在强磁场下其光电子谱劈裂成单态和三重态[3]。

自旋单态的 $SrCu_2(BO_3)_2$ 体系中，在几十特斯拉的强磁场和压力将诱导出分数填充的自旋三重态玻色子[5]。脉冲强磁场下，$Cu^{2+}$离子的核磁共振谱图出现了明显的展宽[6]。

在 $URu_2Si_2$ 中，科学家们发现在 35-39T 之间观察到了一个自旋密度波转变，这将对解决“隐秘序”领域从费米面拓扑学和磁相互作用提出关键一步[10]。在 60T 脉冲强磁场和 4Gpa 高压下，获得了重费米子体系 $CeRh_2Si_2$ 的磁场-压力-温度相图[11]。核磁共振谱则显示，P 掺杂将增强关联温度 T*[12]。

合适的磁场在二类超导体内将引起磁通阵列，科学家通过调节磁场角度，用 6.4-30T 的强磁场诱导出了不同的磁通晶格阵列[13]。他们尝试使用低能中子辐照制造钉扎中心，来增强铁基超导体薄膜材料的最高承载载电流密度，获得了优于低温超导体的数据结果[14]。科学家们还研究了利用应力控制来避免一代银套管铋锶钙铜氧超导体优于磁体失超导致的性能退化[15]，还利用强磁场下的德.哈斯-范.阿尔芬效应表征了超导体 $Ta_4Pd_3Te_{16}$，发现垂直于准一维链方向的一个相变[17]。

科学家们发现，强磁场会导致软物质有机聚合物的极化排列[19]，还会导致锌-锡合金的晶体生长优势面出现不同[23]。科学家们利用激光在 25T 分裂强磁场下，发现了分子的形貌发生了变化，从而改变了性质[9]。

量子霍尔效应是在强磁场下被发现的。科学家们在单层硒化铟薄膜中发现了高迁移率、量子霍尔效应和奇异的光学响应[7]。科学家在化学调控的碳化硅上生长的石墨薄膜制作的霍尔器件中，发现了 v=2 的量子平台，从 5T 一直持续到 80T[8]。科学家们还利用倾斜的强磁场，在铁磁/正常金属双层薄膜中，发现了自旋霍尔磁电阻[24]。

# 目录

最新资讯

## 1. National MagLab racks up new record with hybrid magnet

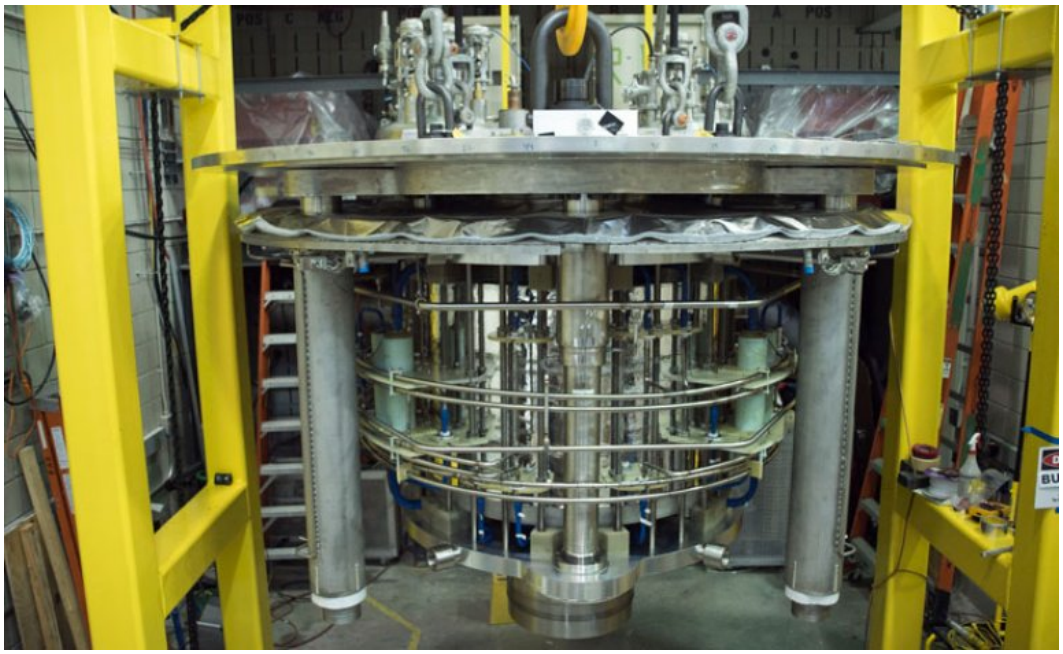

**The world-record 36-tesla series connected hybrid before being lowered into its cryostat**

After a decade of planning, designing and building, the National MagLab has successfully tested the latest addition to its world-record lineup: a 33-ton engineering marvel called the series connected hybrid (SCH) magnet.

On Nov. 8,2016,, the instrument reached its full field, 36 tesla (tesla is a unit of magnetic field strength; a strong refrigerator magnet is .01 tesla, and a typical MRI machine is 1.5 to 3 tesla).

The milestone busts open a door to discovery, making the highest magnetic fields available not just to physicists but, for the first time, to biologists and chemists as well. It was the culmination of 10 years, more than 120,000 person-hours and $18.7 million from the National Science Foundation (NSF) and the state of Florida.

MagLab Flagship Magnets as fllows:

| | **Series Connected Hybrid Magnet** | **45 Tesla Hybrid Magnet** | **900 MHz Ultra-Wide Bore NMR Magnet** |
|---|---|---|---|
| **Height** | 3.6 meters (11.8 feet) | 6.7 meters (22 feet) | About 5 meters (16 feet) |
| **Weight** | 30,000 kg (33 tons) | 31,752 kg (35 tons) | 13,600 kg (15 tons) |
| **Operating temperature** | -269°C (-452°F) | -271°C (-456°F) | -271.45°C (-456.61°F) |
| **Cost to operate at full field** | $678 /hour | $1,452 /hour | $33 /hour |
| **Power required to operate** | 14 Megawatts | 30 Megawatts | 0 Megawatts |

| | | | |
|---|---|---|---|
| **Type of research** | Biology, chemistry and physics | Primarily condensed matter physics | Primarily biology and chemistry |
| **Type of magnet** | Resistive-superconducting hybrid (coils connected in series) | Resistive-superconducting hybrid (coils connected in parallel) | Superconducting |
| **Materials** | Niobium-tin in the superconducting outsert; copper alloys in the resistive insert | Niobium-tin and niobium titanium in the superconducting outsert; copper alloys in the resistive insert | Niobium-tin and Niobium titanium |
| **Frequency** | 1.5 GHz | n/a | 900 MHz |
| **Field strength** | **36 tesla** | **45 tesla** | **21.1 tesla** |
| **Bore size** | 40 mm | 32 mm | 105 mm |
| **Field Homogeneity** | 1 part per million | 150 part per million | 0.001 part per million |
| **Year completed** | 2016 | 1999 | 2004 |
| **Cost** | $18.7 million | $14.4 million | $16 million |

**Information Sources：** https://nationalmaglab.org/news-events/news/national-maglab-racks-up-another-record

## 2. Mini magnet packs world-record, one-two punch

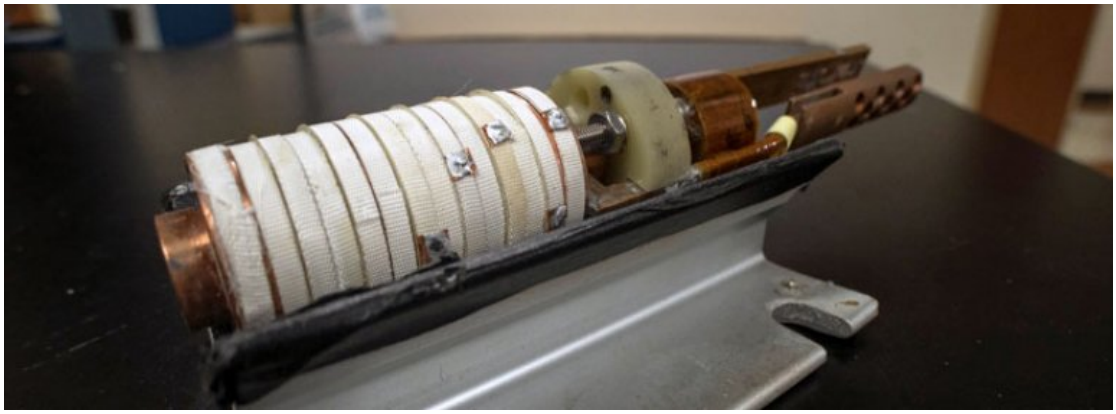

**You could easily hold the 5-cm-long, no-insulation magnet in the palm of your hands**

That was the case January 18 (2017) at the National High Magnetic Field Laboratory when a magnet that fits in the palm of your hand claimed a new world record.

Made of high-temperature superconducting (HTS) tape, the miniature magnet is only the second of its kind ever made. Outperforming its MagLab predecessor, it reached a magnetic field of 11.3 teslas (or T, a unit of magnetic field strength) while inside a larger, 31.2-T resistive magnet. Operating as one 42.5 T "hybrid" magnet, this test instrument achieved two records at once. First, the 42.5 T field is the highest field in which a superconducting magnet has ever operated. Second, 42.5 T is a new world record for an HTS magnet operating within a background field.

The new record was within striking distance of the 45-tesla hybrid magnet, which holds the Guinness World Record for any continuous-field magnet, held by the National MagLab since 1999.

**Information Sources：**https://nationalmaglab.org/news-events/news/mini-magnet-packs-world-record-punch

### 3. €2.3 million for HFML research on strange metals

FOM, the Dutch Foundation for Fundamental Research on Matter, awarded €15.1 million to seven new research programmes that will take off shortly. The 'Strange metals' programme brings together a unique alliance of leading string theorists, quantum many-body theorists, and condensed matter experimentalists from Radboud University and the universities of Amsterdam, Leiden and Utrecht.

The 'Strange metals' research programme, led by Nigel Hussey, director of the Nijmegen High Field Magnet Laboratory, receives €2.3 million from FOM to investigate the origin of this strange metallic behaviour.

The physics of strange metals, which do not conform to the standard models of metallic behaviour, are amongst the most fundamental and pressing problems in modern physics. Strange metals have an electrical resistivity that grows linearly with temperature right up to their melting point. Unlike in conventional systems, however, this linear behaviour terminates not at a single (so-called quantum critical) point at zero temperature, but over an extended range of the phase diagram, implying some form of novel quantum critical phase that defines a genuinely new electronic phase.

The main objective of the Strange Metals programme is to determine whether strange metals represent a novel quantum critical phase whose theory can be described by holographic emergence principles first developed by string theorists in the context of quantum gravity. Furthermore, the scientists aim to advance this 'holographic' theory to the point where real materials can be modelled, and to test both existing and emerging predictions with detailed experimental investigations. Additionally, the consortium will establish the world's first optical apparatus for measuring the optical conductivity of strange metals (and other metals) in high magnetic fields above 35 Tesla at the High Field Magnet Laboratory (HFML).

An identification of the physics behind strange metal behaviour will be an important key step in the development of a coherent theory for high temperature superconductivity, which in turn may provide key guiding principles in our quest for materials with ever higher transition temperatures.

**Information Sources：**http://www.ru.nl/hfml/news/news/news-items/strange-metals/

## 强磁场设备研制

### 1. AC loss evaluation of an HTS insert for high field magnet cooled by cryocoolers

AC losses in a high temperature superconducting (HTS) insert coil for 25-T cryogen-free superconducting magnet during its initial energization are numerically calculated under the assumption

of slab approximation. The HTS insert consisting of 68 single pancakes wound using coated conductors generates a central magnetic field of 11.5 T in addition to the contribution of 14.0 T from a set of low temperature superconducting (LTS) outsert coils. Both the HTS insert and the LTS coils are cooled using cryocoolers, and energized simultaneously up to the central field of 25.5 T with a constant ramp rate for 60 min. The influences of the magnitudes and orientations of locally applied magnetic fields, magnetic interactions between turns and transport currents flowing in the windings are taken into account in the calculations of AC losses. The locally applied fields are separated into axial and radial components, and the individual contributions of these field components to the AC losses are simply summed up to obtain the total losses. The AC losses due to the axial fields become major in the beginning of energization, whereas the total losses monotonically increase with time after the AC losses due to the radial fields become major.

**Information Sources：**http://dx.doi.org/10.1016/j.cryogenics.2016.05.010.

## 2. The 36-T Series-Connected Hybrid Magnet System Design and Integration

The system integration of a 36 T high field resistivesuperconducting hybrid magnet system which will be used primarily for NMR studies is being finalized at the National High Magnetic Field Laboratory in Tallahassee, Florida. The hybrid magnet consists of a 23 T resistive insert coil set nested inside of a 13 T superconducting coil wound with high JC Nb3Sn/Cu cablein- conduit conductor. The resistive and superconducting coils are connected electrically in series and operate at 20 kA. The combined system will enable 1-ppm level uniformity in a 1 cm DSV for condensed-matter NMR at a record level of 1.53 GHz. The resistive insert has four concentric Florida-Bitter coils and operates at 14 MW. The superconducting outsert operates with forced flow supercritical helium at 4.5 K and 3.5 bar. The superconducting protection system consists of two fully independent circuits, one employing voltage averaging comparisons between winding layers and the other a voltage comparison with a co-wound coil. Initial magnet testing of the resistive coils has been completed. The superconducting cold mass has been cooled to 4.5 K and the system is being prepared for combined hybrid magnet testing.

**Information Sources：http://ieeexplore.ieee.org/abstract/document/7742407/?reload=true**

## 3. Role and Impact of the Eddy Current Shield in the LNCMI-G Hybrid Magnet

In the new 43-T LNCMI hybrid magnet, a good conducting shield is inserted between the resistive insert magnet and the superconducting outsert magnet. Its goal is to decrease the ac losses induced in the superconducting conductor during a fault of the insert, disruption of the resistive coils (i.e., fast discharge) by smoothing the flux variations, and avoidance of a

quench of the superconducting coil. The induced currents within the shield are very large due to the presence of copper material, which is the drawback of a good screening effect. Such currents result in large Lorentz forces, particularly during the most severe fault scenario of the resistive insert with the burnout of half of the Bitter coils. Finally, the detection system must be specially designed to handle the effects of the shield on the induced voltages.

**Information Sources：** http://ieeexplore.ieee.org/abstract/document/7403872/

## 强磁场与生物医学

### 1. A new twist on DNA

For DNA to reproduce, its double helix must be made to unwind so that new double helices can be synthesized from each of the two strands. Helicase is the protein "machine" that pulls the two strands apart. Researchers have used the MagLab's 14.5 tesla mass spectrometer to map the contact surfaces when helicase and DNA form a complex, in order to reveal the unwinding mechanism used by the helicase.

Scientists knew that double-stranded DNA is held inside the helicase protein structure. They thought unwound single strands were unconstrained outside the protein. This research revealed that the single strands are in fact tightly held to the helicase protein surface, helping the helicase pull the DNA helix apart from both ends. The information sheds an important light on the fundamental process of cell division.

**Information Sources：** https://nationalmaglab.org/user-facilities/icr/publications-icr/highlights-icr/a-new-twist-on-dna

### 2. New technique for detecting brain tumors

Nuclear magnetic resonance imaging (MRI) is a technique that scientists can use for medical research. It visualizes the distribution of specific atoms in the body. Most of the time MRI maps the hydrogen atoms in the body, which can reveal various abnormalities.

In one hot area of MRI research, scientists are developing ways to map out other atoms in the body besides hydrogen. For example, MagLab researchers have been improving techniques for targeting sodium, which can be used to show how brain tumors respond to chemotherapy.

This research resulted in an important first: The first time that MRI has been used to see oxygen in a living brain, resulting in a relatively clear image, using the MagLab’s 21.1 tesla NMR/MRI magnet. Specifically, it was used to locate a specific isotope of oxygen (oxygen-17,or $^{17}O$, also called enriched oxygen), which had been incorporated into glucose and injected into a living rat.

Isotopes are atoms of the same element that have the same number of protons but different numbers of neutrons, which can result in different properties. Oxygen-16 is by far the most abundant oxygen isotope, but it can't be detected using MRI. So scientists manufactured glucose (the form of sugar used by our cells) with $^{17}O$, which *can* be detected using MRI. They then injected it into rats that had cancerous brain tumors, which consume a lot of glucose.

When the researchers did MRI scans of the animals that searched for the $^{17}O$ from the injected glucose, they confirmed its appearance in the rats' brains, effectively identifying the location of the tumor.

**Information Sources：** https://nationalmaglab.org/user-facilities/nmr-mri/publications-nmr-mri/highlights-nmr-mri/detecting-brain-tumors

## 强磁场与材料科学

### 1. Chirality of graphene electrons manipulated by high magnetic fields

Electrons have various basic properties: they have a charge, a spin, and on top of that can have an additional degree of freedom: their pseudospin or valley degeneracy, which corresponds to their location in the atomic structure. In graphene, the truly two-dimensional form of carbon, two types of electrons with an opposite pseudospins exist. It is either parallel or antiparallel to its direction of propagation and is therefore referred to as chirality. However, measuring an electron's chirality has proven to be quite tricky. And to base calculations on it, for example when developing a future quantum computer, scientists need to be able to observe and manipulate the electrons' chirality. In the current publication, scientists from the the University of Manchester, the University of Nottingham and two labs of the European High Magnetic Field Laboratories (EMFL), the High Field Magnet Laboratory (HFML) in Nijmegen and the Laboratoire National des Champs Magnétiques Intenses (LNCMI) in Grenoble, achieved both.

They constructed special structures of stacked graphene with a thin layer of boron nitride in between. The hexagonal graphene molecules were almost perfectly aligned, but not completely. Electrons can flow from the top graphene layer to the bottom one by quantum mechanical tunnelling though the insulation boron nitride layer between them. However, since the graphene layers a slightly misaligned this current flow is difficult because electrons have to displace laterally from one molecule to the next. High magnetic fields of up to 30 Tesla, applied in the plane of the graphene, can help the electrons make this 'jump', by giving them a so-called Lorentz boost, i.e. by changing their direction of movement slightly when passing through the boron nitride. Additionally, this makes it possible to select, depending on the angle of the magnetic field, one specific chirality which can tunnel easily thought the boron nitride whereas the other one is suppressed.

'Making these specific graphene structures, a kind of tiny electronic sandwiches, is a complicated and time-consuming process', says Uli Zeitler, a physicist at the HFML. 'The samples in this study were made at the National Graphene Institute of the University of Manchester, and we subsequently exposed them to a high magnetic field of 30 tesla. Currently, there are some ten to twenty two-dimensional materials that resemble graphene and can be stacked to so-called van-der-Waals heterostructures. These allow us to access and to control properties in a way not possible in traditional semiconductors, and that is why they have our attention. By building and investigating these sandwiches, in the end we can build small electronic devices with specific properties. This is interesting for e.g. valleytronics, a new scientific field where researchers aim to store information in the pseudospins of electrons, which may have important implications on a future quantum computer.'

**Information Sources**：http://www.emfl.eu/single/newsartikel/chirality-of-graphene-electrons-manipulated-by-high-magnetic-fields.html

## 2. Tuning the valley and chiral quantum state of Dirac electrons in van der Waals heterostructures

Chirality is a fundamental property of electrons with the relativistic spectrum found in graphene and topological insulators. It plays a crucial role in relativistic phenomena, such as Klein tunneling, but it is difficult to visualize directly. Here, we report the direct observation and manipulation of chirality and pseudospin polarization in the tunneling of electrons between two almost perfectly aligned graphene crystals. We use a strong in-plane magnetic field as a tool to resolve the contributions of the chiral electronic states that have a phase difference between the two components of their vector wave function. Our experiments not only shed light on chirality, but also demonstrate a technique for preparing graphene's Dirac electrons in a particular quantum chiral state in a selected valley.

**Information Sources**：http://science.sciencemag.org/content/353/6299/575

## 3. Trion fine structure and coupled spin-valley dynamics in monolayer tungsten disulfide

Monolayer transition-metal dichalcogenides have recently emerged as possible candidates for valleytronic applications, as the spin and valley pseudospin are directly coupled and stabilized by a large spin splitting. The optical properties of these two-dimensional crystals are dominated by tightly bound electron–hole pairs (excitons) and more complex quasiparticles such as charged excitons (trions). Here we investigate monolayer WS2 samples via photoluminescence and time-resolved Kerr rotation. In photoluminescence and in energy-dependent Kerr rotation measurements, we are able to resolve two different trion states, which we interpret as intravalley and intervalley trions. Using

time-resolved Kerr rotation, we observe a rapid initial valley polarization decay for the A exciton and the trion states. Subsequently, we observe a crossover towards exciton–exciton interaction-related dynamics, consistent with the formation and decay of optically dark A excitons. By contrast, resonant excitation of the B exciton transition leads to a very slow decay of the Kerr signal.

**Information Sources：** http://www.nature.com/articles/ncomms12715

## 4. Magnetic torque anomaly in the quantum limit of Weyl semimetals（New technique for identifying Weyl materials）

This research was conducted in the 65 T pulsed magnet at the MagLab's Pulsed Field Facility located at Los Alamos and 45 T Hybrid at DC Field Facility located at Tallahassee.

Electrons in materials with linear dispersion behave as massless Weyl- or Dirac-quasiparticles, and continue to intrigue due to their close resemblance to elusive ultra-relativistic particles as well as their potential for future electronics. Yet the experimental signatures of Weyl-fermions are often subtle and indirect, in particular if they coexist with conventional, massive quasiparticles. Here we show a pronounced anomaly in the magnetic torque of the Weyl semimetal NbAs upon entering the quantum limit state in high magnetic fields. The torque changes sign in the quantum limit, signalling a reversal of the magnetic anisotropy that can be directly attributed to the topological nature of the Weyl electrons. Our results establish that anomalous quantum limit torque measurements provide a direct experimental method to identify and distinguish Weyl and Dirac systems.

**Information Sources：** http://www.nature.com/articles/ncomms12492?WT.feed_name=subjects_topological-insulators

## 5. Crystallization of spin superlattices with pressure and field in the layered magnet $SrCu_2(BO_3)_2$

An exact mapping between quantum spins and boson gases provides fresh approaches to the creation of quantum condensates and crystals. Here we report on magnetization measurements on the dimerized quantum magnet $SrCu_2(BO_3)_2$ at cryogenic temperatures and through a quantum-phase transition that demonstrate the emergence of fractionally filled bosonic crystals in mesoscopic patterns, specified by a sequence of magnetization plateaus. We apply tens of Teslas of magnetic field to tune the density of bosons and gigapascals of hydrostatic pressure to regulate the underlying interactions. Simulations help parse the balance between energy and geometry in the emergent spin superlattices. The magnetic crystallites are the end result of a progression from a direct product of singlet states in each short dimer at zero field to preferred filling fractions of

spin-triplet bosons in each dimer at large magnetic field, enriching the known possibilities for collective states in both quantum spin and atomic systems.

**Information Sources：** http://www.nature.com/articles/ncomms11956

## 6. Pulsed-field broadband NMR of SrCu2(BO3)2

In this material, electronic spins of $Cu^{2+}$ ions within the $Cu_2(BO_3)_2$ layers form a lattice of mutually orthogonal spin-singlet dimers with significant interdimer interaction, giving rise to pronounced magnetic frustration. At high magnetic fields, triplet states with reduced kinetic energy condense, resulting in a field-driven sequence of magnetic superlattices with corresponding plateaus in the macroscopic magnetization. The microscopic detection of these superlattice structures by means of NMR as a local probe is of great interest. To study all magnetization plateaus up to half of the saturation value, pulsed magnetic fields up to the regime of 100 T are required. A team of Estonian, Canadian, and German scientists from Leipzig University, the NICPB (Tallinn), McMaster University (Hamilton), and the HLD has performed NMR measurements on $SrCu_2(BO_3)_2$ in pulsed magnetic fields. The results are in very good agreement with a transition from a high-temperature, paramagnetic state to a low-temperature, commensurate superstructure of field-induced spin-dimer triplets in the 1/3 magnetization plateau. Moreover, the technical approach to measure broadband NMR in pulsed fields, that was developed in the course of this work, opens the door not only to the exploration of the higher-field ground states of $SrCu_2(BO_3)_2$, but also to studies of many other quantum magnets with complex interactions that stabilize new phases of matter in very strong magnetic fields.

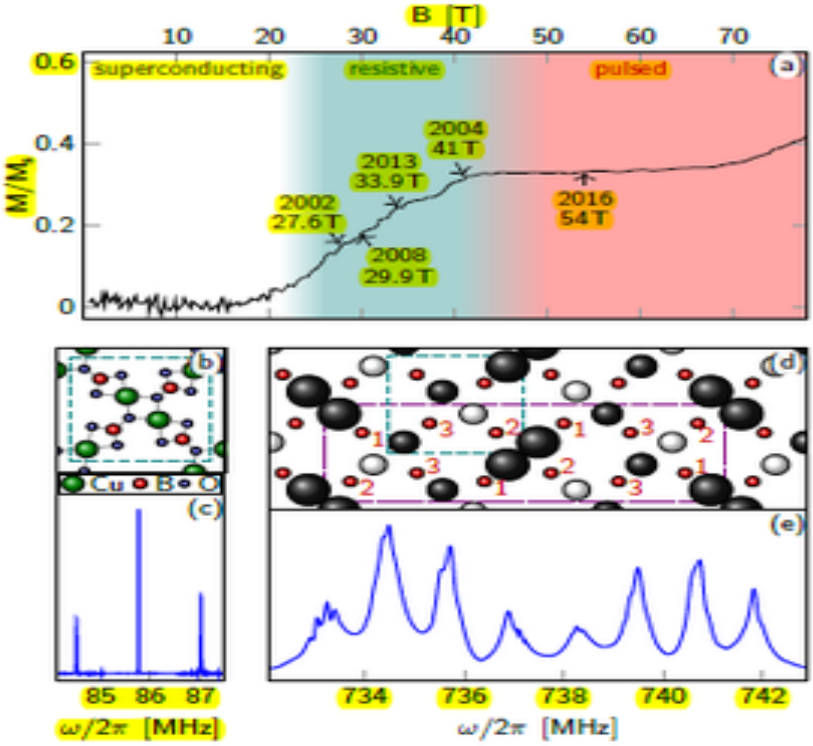


*(a) Macroscopic magnetization of $SrCu_2(BO_3)_2$ at 2 K (from Matsuda et al.). (b) Unit cell of the $Cu_2(BO_3)_2$ plane and (c) the corresponding $^{11}B$ NMR spectrum at 6 T and 5 K. (d) Magnetic superlattice in the 1/3 magnetization plateau with three different 11B sites (red spheres). White and black spheres represent negative and positive spin polarization, their size the magnitude. (e) $^{11}B$ NMR spectrum at 54 T and 2 K.*

**Information Sources:** http://www.emfl.eu/single/newsartikel/pulsed-field-broadband-nmr-of-srcu2bo32.html

## 7. High electron mobility, quantum Hall effect and anomalous optical response in atomically thin InSe.

A decade of intense research on two-dimensional (2D) atomic crystals has revealed that their properties can differ greatly from those of the parent compound. These differences are governed by changes in the band structure due to quantum confinement and are most profound if the underlying lattice symmetry changes. Here we report a high-quality 2D electron gas in few-layer InSe encapsulated in hexagonal boron nitride under an inert atmosphere. Carrier mobilities are found to exceed $10^3$ $cm^2$ $V^{-1}$ $s^{-1}$ and $10^4$ $cm^2$ $V^{-1}$ $s^{-1}$ at room and liquid-helium temperatures, respectively, allowing the observation of the fully developed quantum Hall effect. The conduction electrons occupy a single 2D subband and have a small effective mass. Photoluminescence spectroscopy reveals that the bandgap increases by more than 0.5 eV with decreasing the thickness from bulk to bilayer InSe. The band-edge optical response vanishes in monolayer InSe, which is attributed to the monolayer's

mirror-plane symmetry. Encapsulated 2D InSe expands the family of graphene-like semiconductors and, in terms of quality, is competitive with atomically thin dichalcogenides and black phosphorus.

**Information Sources：** http://www.nature.com/nnano/journal/vaop/ncurrent/full/nnano.2016.242.html

## 8. Puddle-Induced Resistance Oscillations in the Breakdown of the Graphene Quantum Hall Effect.

We report on the stability of the quantum Hall plateau in wide Hall bars made from a chemically gated graphene film grown on SiC. The ν=2 quantized plateau appears from fields B≃5 T and persists up to B≃80 T. At high current density, in the breakdown regime, the longitudinal resistance oscillates with a 1/B periodicity and an anomalous phase, which we relate to the presence of additional electron reservoirs. The high field experimental data suggest that these reservoirs induce a continuous increase of the carrier density up to the highest available magnetic field, thus enlarging the quantum plateaus. These in-plane inhomogeneities, in the form of high carrier density graphene pockets, modulate the quantum Hall effect breakdown and decrease the breakdown current.

**Information Sources：** https://journals.aps.org/prl/abstract/10.1103/PhysRevLett.117.237702

## 9. Anomalous Increase in Nematic-Isotropic Transition Temperature in Dimer Molecules Induced by a Magnetic Field

This research was conducted in the 25T Split Helix Magnet (cell 5) at the MagLab's DC Field Facility.

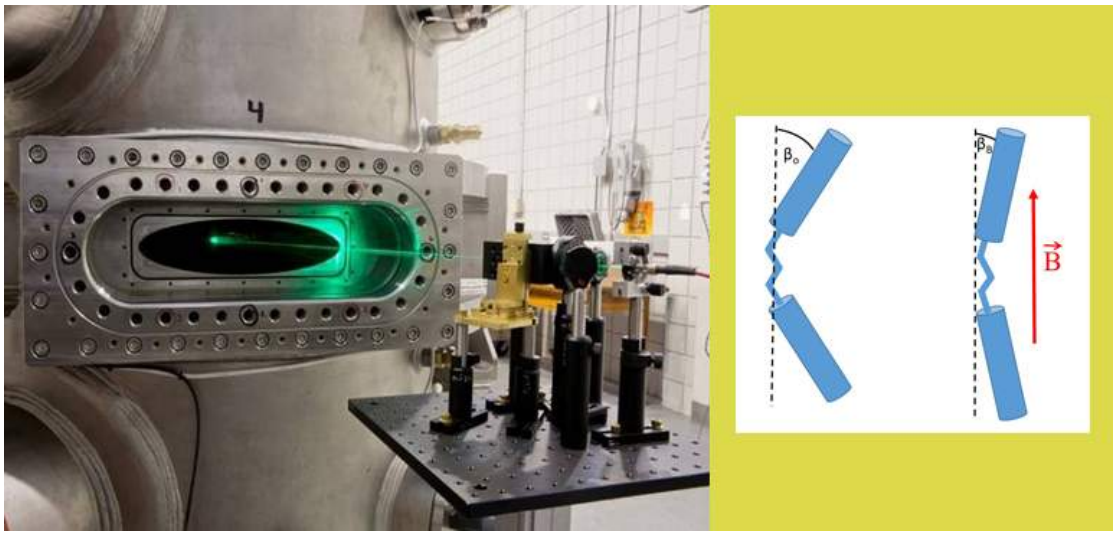


Using lasers in the split helix magnet (above), scientists observed high magnetic fields change the shape of molecules, thereby changing some of their properties.

We have determined the nematic-isotropic transition temperature as a function of an applied magnetic field in three different thermotropic liquid crystalline dimers. These molecules are comprised

of two rigid calamitic moieties joined end to end by flexible spacers with odd numbers of methylene groups. They show an unprecedented magnetic field enhancement of nematic order in that the transition temperature is increased by up to 15 K when subjected to a 22 T magnetic field. The increase is conjectured to be caused by a magnetic-field-induced decrease of the average bend angle in the aliphatic spacers connecting the rigid mesogenic units of the dimers.

**Information Sources：** http://journals.aps.org/prl/abstract/10.1103/PhysRevLett.116.217801

## 10. Field-induced spin-density wave beyond hidden order in $URu_2Si_2$

Under a high magnetic field applied along c, a cascade of first-order phase transitions leads to a polarized paramagnetic regime above μ0H3 = 39 T. Here, thanks to a new cryomagnet (developed by the EMFL-Toulouse, the CEA-Grenoble, and the ILLGrenoble) allowing neutron diffraction up to 40 T, we have determined that URu2Si2 enters in a spin-density wave state in fields between 35 and 39 T. The transition to the spin-density wave represents a unique touchstone for understanding the hidden-order phase. The Figure shows the diffracted neutron intensities recorded in magnetic fields up to 40 T at the momentum transfers Q = (0.6 0 0) and (1.6 0 -1), which are satellites of wavevector k1 = Q – τ = (0.6 0 0) around the structural Bragg positions τ = (0 0 0) and (1 0 -1), respectively. The enhancement of the intensity at 2 K, absent at 18 K, shows that the spin-density wave with wavevector k1 is established at high field and low temperature. In an itinerant picture of magnetism, a spin-density wave can be related to a partial or complete nesting of two parts of the Fermi surface. In URu2Si2, our observation of a spin-density wave in magnetic fields between 35 and 39 T will certainly push to develop models incorporating on equal basis the Fermi-surface topology and the magnetic interactions. To describe competing quantum instabilities between the hidden-order and long-range-ordered phases, such models will be a basis to solve the hidden-order puzzle.

**Information Sources：** http://www.emfl.eu/single/newsartikel/field-induced-spin-density-wave-beyond-hidden-order-in-uru2si2.html

## 11. Three-dimensional critical phase diagram of the Ising antiferromagnet $CeRh_2Si_2$ under intense magnetic field and pressure

Using novel instrumentation to combine extreme conditions of intense pulsed magnetic field up to 60 T and high pressure up to 4 GPa, we have established the three-dimensional (3D) magnetic field-pressure-temperature phase diagram of a pure stoichiometric heavy-fermion antiferromagnet (CeRh2Si2). We find a temperature- and pressure-dependent decoupling of the critical and pseudometamagnetic fields at the borderlines of antiferromagnetism and strongly-correlated paramagnetism. This 3D phase diagram is representative of a class of heavy-fermion Ising

antiferromagnets, where long-range magnetic ordering is decoupled from a maximum in the magnetic susceptibility. The combination of extreme conditions enabled us to characterize different quantum phase transitions, where peculiar quantum critical properties are revealed. The interest to couple the effects of magnetic field and pressure on quantum-critical correlated-electron systems is stressed.

**Information Sources：** https://journals.aps.org/prb/abstract/10.1103/PhysRevB.95.014411

## 12. NMR investigation of antiferromagnetism and coherence in $URu_2Si_{2-x}P_x$

We report $^{31}P$ and $^{29}Si$ NMR in single crystals of $URu_2Si_{2-x}P_x$ for x = 0.09 and x = 0.33. The spectra in the x = 0.33 sample are consistent with a homogenous commensurate antiferromagnetic phase below $T_N \sim 37$ K. The Knight shift exhibits an anomaly at the coherence temperature $T^*$ that is slightly enhanced with P doping. Spin-lattice-relaxation rate data indicate that the density of states is suppressed for x = 0.09 below 30 K, similar to the undoped compound, but there is no evidence of long-range order at this concentration. Our results suggest that Si substitution provides chemical pressure and electronic tuning mediated by filling of the s/p shells with minimal electronic inhomogeneity.

**Information Sources：** http://journals.aps.org/prb/abstract/10.1103/PhysRevB.95.041107

## 13. Magnetic-field-induced vortex-lattice transition in HgBa2CuO4+δ

Measurements of the 17O nuclear magnetic resonance (NMR) quadrupolar spectrum of apical oxygen in HgBa2CuO4+δ were performed over a range of magnetic fields from 6.4–30 T in the superconducting state. Oxygen-isotope-exchanged single crystals were investigated with doping corresponding to superconducting transition temperatures from 74 K underdoped, to 78 K overdoped. The apical oxygen site was chosen since its NMR spectrum has narrow quadrupolar satellites that are well separated from any other resonance. Nonvortex contributions to the spectra can be deconvolved in the time domain to determine the local magnetic field distribution from the vortices. Numerical analysis using Brandt's Ginzburg-Landau theory was used to find structural parameters of the vortex lattice, penetration depth, and coherence length as a function of magnetic field in the vortex solid phase. From this analysis we report a vortex structural transition near 15 T from an oblique lattice with an opening angle of 73◦ at low magnetic fields to a triangular lattice with 60◦ stabilized at high field. The temperature for onset of vortex dynamics has been identified from spin-spin relaxation. This is independent of the magnetic field at sufficiently high magnetic field similar to that reported for YBa2Cu3O7 and Bi2Sr2CaCu2O8+δ and is correlated with mass anisotropy of the material. This behavior is accounted for theoretically only in the limit of very high anisotropy.

**Information Sources：** https://journals.aps.org/prb/pdf/10.1103/PhysRevB.95.024512

## 14. Enhancing the superconducting properties of an iron-based material

Scientists pioneer method that enables material to carry more electrical current without resistance at a higher temperature.

Iron-based superconductors can conduct electricity without resistance at unusually high temperatures relative to those of conventional superconductors, which must be chilled to near absolute zero (minus 459 degrees Fahrenheit) to release their superconducting powers. In addition, they're relatively easy to bend and can carry electrical current easily in different directions under high magnetic fields before superconductivity becomes suppressed. These characteristics make iron-based superconductors promising for advanced energy applications, from electric vehicles to wind turbines and medical imaging devices. However, the amount of current they can carry has been low in comparison to other superconductors. Scientists have been trying to increase this amount, but doing so has often come at the cost of degrading another key superconducting property—the critical temperature at which superconductivity emerges.

Now, a team of scientists has come up with a way to double the amount of electrical current an iron-based material can carry without losing its superconducting properties, while increasing the material's critical temperature. Their method, reported in a paper published today in Nature Communications, makes use of a readily available technology that could be used to improve the performance of superconducting wires and tapes.

"By bombarding the material with protons at low energy, we simultaneously increased the material's current-carrying capacity and critical temperature — the first time that this has been possible in an iron-based superconductor," said physicist Qiang Li, head of the Advanced Energy Materials Group at the U.S. Department of Energy's (DOE) Brookhaven National Laboratory, who directed the research. "There are low-energy ion facilities all over the world that can do this inexpensively."

Shooting ions at superconducting materials is a well-established method for artificially introducing defects in the crystal structure or chemistry of the materials to increase the amount of current they can carry. These defects "pin" in place, or trap, the microscopic magnetic vortices that form when the superconductor is placed in a strong magnetic field, such as those generated by magnets in magnetic resonance imaging (MRI) machines. If free to move around, the vortices dissipate energy, thereby destroying the superconductor's ability to carry electrical current without energy loss.

Unfortunately, if the defects produced by ion irradiation create too much disorder in the superconductor, they lower its critical temperature. Because superconductors currently require extreme cooling to conduct electricity without resistance, any decrease in the critical temperature is undesirable.

In a Goldilocks sense, the defects must be "just right" — not too big, not too small. Scientists can design such defects by selecting the appropriate ion species (e.g., protons, gold ions, argon ions) and ion energy.

"Some ions or energies may cause large enough damage to interfere with superconductivity, while others may not produce any effect at all," explained coauthor Toshinori Ozaki, a former scientist in Brookhaven Lab's Advanced Energy Materials Group who is now a faculty member at Japan's Kwansei Gakuin University. "So we run simulations to figure out what combination should produce the optimal defect—one that can hold down the magnetic vortices without negatively impacting the material's superconducting properties."

In the case of the iron-based material the team studied, low-energy protons did the trick. Using electron microscopes, the scientists took images of the thin films (about 100 nanometers thick) of the material they prepared, before and after they hit the films with low-energy protons.

"Throughout the irradiated films, we saw individual chains of defects created by the collisions between the incident ions and nucleus that broke the perfect atomic order, causing the lattice to locally compress or stretch out," said coauthor Lijun Wu, a materials scientist at Brookhaven who led the microscopy work.

In a performance check in one of the 35 tesla magnets in the MagLab's DC Field Facility, the scientists measured the amount of electrical current running through the films in low and high magnetic fields. In high fields, the irradiated films carried more current than any low-temperature superconductor. This result suggests that the defects and local lattice strain must be strongly pinning the magnetic vortices that would otherwise impede the flow of current.

“The work done by Qiang Li and co-workers is a great example of the user-driven, multi-disciplinary, materials research efforts at the National MagLab that seek to innovate new materials and enhance the performance of existing ones," said DC Field Director Tim Murphy.

To figure out what caused the surprising increase in the critical temperature, the team created a strain "map" that laid out where the locally compressed and tensile (stretched out) regions were located. Previous studies had already shown that the type of lattice strain correlates with the critical temperature: highly compressed regions with a high critical temperature, and highly tensile regions with a low critical temperature. In the team's films, the compressive ones took up much more space, leading to an overall raised critical temperature.

According to Li, these performance gains are only the beginning: "We believe that the critical current and temperature can be further enhanced by fine tuning the structure of the defects and the arrangement of the lattice strains."

This work was supported by the DOE Office of Science. Scientists performed the high-field

measurements at the National High Magnetic Field Laboratory at Florida State University. Brookhaven scientists used polishing tools at the Center for Functional Nanomaterials, a DOE Office of Science User Facility, to prepare the films for electron microscopy.

**Information Sources：** https://nationalmaglab.org/news-events/news/enhancing-the-superconducting-properties-of-an-iron-based-material

## 15. Strain control of composite superconductors to prevent degradation of superconducting magnets due to a quench: I. Ag/ $Bi_2Sr_2CaCu_2O_x$ multifilament round wires

The critical current of many practical superconductors is sensitive to strain, and this sensitivity is exacerbated during a quench that induces a peak local strain which can be fatal to superconducting magnets. Here, a new method is introduced to quantify the influence of the conductor stress and strain state during normal operation on the margin to degradation during a quench, as measured by the maximum allowable hot spot temperature $T_{allowable}$, for composite wires within superconducting magnets. The first conductor examined is Ag-sheathed $Bi_2Sr_2CaCu_2O_x$ round wire carrying high engineering critical current density, $J_E$, of 550 A $mm^{-2}$ at 4.2 K and 15 T. The critical axial tensile stress of this conductor is determined to be 150 MPa and, in the absence of Lorentz forces, $T_{allowable}$ is greater than 450 K. With increasing axial tensile stress, $\sigma_a$, however, $T_{allowable}$ decreases nonlinearly, dropping to 280 K for $\sigma_a = 120$ MPa and to 160 K for $\sigma_a = 145$ MPa. $T_{allowable}(\sigma_a)$ is shown to be nonlinear and independent of magnetic field from 15 to 30 T. $T_{allowable}(\sigma_a)$ dictates the balance between magnetic field generation, which increases with the magnet operating current and stress, and the safety margin, which decreases with decreasing $T_{allowable}$, and therefore has important engineering value. It is also shown that $T_{allowable}(\sigma_a)$ can be predicted accurately by a general strain model, showing that strain control is the key to preventing degradation of superconductors during a quench.

**Information Sources：** http://iopscience.iop.org/article/10.1088/0953-2048/30/2/025005/meta

## 16. Broken rotational symmetry on the Fermi surface of a high-Tc superconductor

Broken fourfold rotational ($C_4$) symmetry is observed in the experimental properties of several classes of unconventional superconductors. It has been proposed that this symmetry breaking is important for superconducting pairing in these materials, but in the high-$T_c$ cuprates this broken symmetry has never been observed on the Fermi surface. Here we report a pronounced anisotropy in the angle dependence of the interlayer magnetoresistance of the underdoped high transition temperature (high-$T_c$) superconductor $YBa_2Cu_3O_{6.58}$, directly revealing broken $C_4$ symmetry on the Fermi surface. Moreover, we demonstrate that this Fermi surface has $C_2$ symmetry of the type

produced by a uniaxial or anisotropic density-wave phase. This establishes the central role of $C_4$ symmetry breaking in the Fermi surface reconstruction of $YBa_2Cu_3O_{6+\delta}$, and suggests a striking degree of universality among unconventional superconductors.

**Information Sources：** http://www.nature.com/articles/s41535-017-0013-z

## 17. Thermodynamic anomaly above the superconducting critical temperature in the quasi-one-dimensional superconductor $Ta_4Pd_3Te_{16}$

We study the intrinsic electronic anisotropy and fermiology of the quasi-one-dimensional superconductor $Ta_4Pd_3Te_{16}$. Below $T * = 20$ K, we detect a thermodynamic phase transition that predominantly affects the conductivity perpendicular to the quasi-one-dimensional chains. The transition relates to the presence of charge order that precedes superconductivity. Remarkably, the Fermi surface pockets detected by de Haas–van Alphen oscillations are unaffected by this transition, suggesting that the ordered state does not break any translational symmetries but rather alters the scattering of the quasiparticles themselves.

**Information Sources：** https://journals.aps.org/prb/abstract/10.1103/PhysRevB.95.075121

## 18. Magnetic Resonance Microscopy (MRM) of Single Mammalian Myofibers and Myonuclei

Recently, the first magnetic resonance microscopy (MRM) images at the cellular level in isolated mammalian brain tissues were obtained using microsurface coils. These methods can elucidate the cellular origins of MR signals and describe how these signals change over the course of disease progression and therapy. In this work, we explore the capability of these microimaging techniques to visualize mouse muscle fibers and their nuclei. Isolated myofibers expressing lacZ were imaged with and without a stain for β-galactosidase activity (S-Gal + ferric ammonium citrate) that produces both optical and MR contrast. We found that MRM can be used to image single myofibers with 6-μm resolution. The ability to image single myofibers will serve as a valuable tool to study MR properties attributed to healthy and myopathic cells. The ability to image nuclei tagged with MR/Optical gene markers may also find wide use in cell lineage MRI studies.

**Information Sources：** http://www.nature.com/articles/srep39496

## 19. Polarization of Soft Materials through Magnetic Alignment of Polymeric Organogels under Low-Field Conditions

Through application of an external magnetic field upon jellification of poly(3-hydroxybutyric acid-co-3-hydroxyvaleric) acid (PHBV) polymer in different solvents, an anisotropic organogel is

obtained. This material presents two alignment steps in an external magnetic field, in the liquid phase and during the jellification, both phenomena measured by magnetic field induced linear birefringence. Remarkably, the organogel developed in this study presents a strong level of birefringence, 80% of its maximum, in an external magnetic field as low as 2 T resulting from the magnetic alignment of the fibers of the material. This anisotropic material shows changes of absorbance upon rotation of a polarizer switching from transparent to opaque. In addition, its suprastructure does not influence the luminescent properties of encapsulated chromophores, allowing the formation of colored anisotropic materials.

**Information Sources：** http://pubs.acs.org/doi/abs/10.1021/acs.chemmater.6b02687

## 20. Excitonic Valley Effects in Monolayer WS2 under High Magnetic Fields

Transition-metal dichalcogenides can be easily produced as atomically thin sheets, exhibiting the possibility to optically polarize and read out the valley pseudospin of extremely stable excitonic quasiparticles present in these 2D semiconductors. Here, we investigate a monolayer of tungsten disulfide in high magnetic fields up to 30 T via photoluminescence spectroscopy at low temperatures. The valley degeneracy is lifted for all optical features, particularly for excitons, singlet and triplet trions, for which we determine the g factor separately. While the observation of a diamagnetic shift of the exciton and trion resonances gives us insight into the real-space extension of these quasiparticles, magnetic field-induced valley polarization effects shed light onto the exciton and trion dispersion relations in reciprocal space. The field dependence of the trion valley polarizations is in line with the predicted trion splitting into singlet and triplet configurations.

**Information Sources：** http://pubs.acs.org/doi/abs/10.1021/acs.nanolett.6b04171

## 21. de Haas–van Alphen study of role of 4 f electrons in antiferromagnetic CeZn 11 as compared to its nonmagnetic analog LaZn 11

We present a de Haas–van Alphen study of the Fermi surface of the low-temperature antiferromagnet CeZn11 and its nonmagnetic analog LaZn11, measured by torque magnetometry up to fields of 33T and at temperatures down to 320mK. Both systems possess similar de Haas–van Alphen frequencies, with three clear sets of features—ranging from 50T to 4kT—corresponding to three bands of a complex Fermi surface, with an expected fourth band also seen weakly in CeZn11. The effective masses of the charge carriers are very light (<1me) in LaZn11 but a factor of 2–4 larger in CeZn11, indicative of stronger electronic correlations. We perform detailed density functional theory (DFT) calculations for CeZn11 and find that only DFT+U calculations with U=1.5eV, which localize the 4f states, provide a good match to the measured de Haas–van Alphen frequencies, once the presence of

magnetic breakdown orbits is also considered. Our study suggests that the Fermi surface of CeZn11 is very close to that of LaZn11 being dominated by Zn 3d, as the Ce 4f states are localized and have little influence on its electronic structure, however, they are responsible for its magnetic order and contribute to enhance electronic correlations.

**Information Sources：**https://journals.aps.org/prb/abstract/10.1103/PhysRevB.94.235103

## 22. The Effect of High Magnetic Field on Electromagnetic Response and Microwave Absorption of Cobalt Particles During Annealing Process

The effect of high magnetic field on microwave absorption of cobalt particles, dispersed uniformly in a paraffin matrix, was investigated in microwave range of 2–18 GHz. The high magnetic field during annealing process could significantly improve the dielectric loss of cobalt particles. The maximum reflection loss of the cobalt particles annealed in high magnetic field is −25.00 dB while the coating thickness is 2.5 mm, which is raised by 62.87 % compared with the ones annealed without high magnetic field. The enhancement in microwave absorption may be ascribed to the improved dielectric loss of cobalt particles induced by high magnetic field.

**Information Sources：**https://link.springer.com/article/10.1007%2Fs10948-016-3686-9

## 23. Crystallographic growth pattern of zinc-rich plate-like cells under a high magnetic field

The high magnetic field induced regularly aligned zinc-rich plate-like cells during solidification of a Zn-27.6 wt.%Sn alloy were investigated, along with the detailed analysis of crystallographic growth pattern. The results show that such plate-like cells were formed three-dimensionally and grew in the following pattern: a) a crystal grew out of the {0001} basal plane to form the horizontally extended primary trunks; b) the primary trunks branched vertically and then produced the primary trunks; c) the primary trunks branched again in the {0001} basal plane and created the high-order arms, some of which then grew out of the {0001} basal plane for the next growth cycle. In such a repeated manner, a plate-like cell was finally formed.

**Information Sources：**http://dx.doi.org/10.1016/j.matlet.2016.09.013

## 24. Spin Hall magnetoresistance in a canted ferrimagnet

We study the spin Hall magnetoresistance effect in ferrimagnet/normal metal bilayers, comparing the response in collinear and canted magnetic phases. In the collinear magnetic phase, in which the sublattice magnetic moments are all aligned along the same axis, we observe the conventional spin Hall magnetoresistance. In contrast, in the canted phase, the magnetoresistance changes sign. Using

atomistic spin simulations and x-ray absorption experiments, we can understand these observations in terms of the magnetic field and temperature dependent orientation of magnetic moments on different magnetic sublattices. This enables a magnetotransport based investigation of noncollinear magnetic textures.

**Information Sources：** https://journals.aps.org/prb/abstract/10.1103/PhysRevB.94.094401

## 版权及合理使用声明



**联系方式：**

**邮箱：shenfei@iim.ac.cn**

**电话：0551-65595332**